Spin transitions induced by a magnetic field in quantum dot molecules

Ramin M. Abolfath[1,2] and Pawel Hawrylak[1]
[1]*Institute for Microstructural Sciences, National Research Council of Canada, Ottawa, Canada K1A 0R6*
[2]*Department of Radiation Oncology, University of Texas Southwestern Medical Center, Dallas, Texas 75390, USA*
(Received 4 March 2008; revised manuscript received 28 March 2008; published 29 April 2008)

We present a theoretical study on magnetic field driven spin transitions of electrons in coupled lateral quantum dot molecules. A detailed study of spin phases of artificial molecules composed of two laterally coupled quantum dots with $N=8$ electrons are presented as a function of magnetic field, Zeeman energy, and detuning by using a real space Hartree–Fock configuration interaction technique. A microscopic picture of a quantum Hall ferromagnet corresponding to zero and full spin polarization at filling factors $\nu=2$ and $\nu=1$, and ferrimagnetic phases, resulting from coupling of the two dots, is presented.

DOI: 10.1103/PhysRevB.77.165430 PACS number(s): 73.43.Lp, 73.63.Kv, 75.50.Gg

I. INTRODUCTION

The application of a spin of electrons in quantum dots for the generation of electron entanglement and quantum information processing in solid state devices is of current experimental[1–11] and theoretical interest.[14–20] Controlling the spin of electrons in single quantum dots by tuning the external magnetic field, the confining potential, the number of electrons, and the Zeeman coupling has been demonstrated.[2–7] It was shown that in a strong magnetic field, electrons form a spin singlet quantum Hall droplet at a filling factor $\nu=2$. Increasing the magnetic field leads to the spin-flip transitions until the spin polarized filling factor $\nu=1$ droplet is reached.[2] Spin flips beyond the first spin flip are associated with correlated states such as spin biexcitons, which are identified and observed experimentally.[5] Quantum dot molecules offer an additional possibility of coupling and controlling spin transitions by tuning the tunneling barrier, which controls the interdot coupling.[14,18–21] The recently demonstrated time dependent control of the tunneling barrier height and confining potential,[6] and the quantum state of the electron spin by applying an oscillating magnetic field (Rabi oscillations),[7] resulted in a coherent manipulation of two electron spins in coupled quantum dot molecules. Recent experiments by Pioro-Ladriere *et al.* in Ref. 3 suggested that in a strong magnetic field, electrons are expected to form a quantum Hall droplet in each quantum dot. The edge states of each droplet can be coupled in a controlled way by using barrier electrodes and, at filling factor $\nu=2$, effectively reduce the many-electron double dot system to a two-level molecule.[3] When populated with one electron each, one expects to have singlet-triplet transitions of two valence electrons in the background of core electrons of the spin singlet $\nu=2$ droplets. With increasing magnetic field, transitions to higher spin polarized states is expected, where coupled quantum dots resemble artificial magnetic molecules.

In this paper, we investigate the effect of the interdot tunneling and electron-electron interactions on the evolution of the total spin of electrons in a quantum dot molecule as a function of electron numbers and magnetic field. We study the many-body effects in the spin-flip transitions by systematically incorporating the interdot and intradot electron-electron Coulomb interactions using real space Hartree–Fock configuration interaction (HF-CI) technique. We find quantum Hall droplets with zero and full polarization, which are identified as $\nu=2$ and $\nu=1$ quantum Hall droplets[14] in analogy to single quantum dots and quantum Hall ferromagnetism.[22] Between these two states, we find a series of continuous transitions among partially spin polarized phases. These partially polarized phases correspond to spin flips. A simultaneous spin flip in each isolated dot must lead to an even number of spin flips in a double dot. Recently, we have found partially polarized phases that correspond to an odd number of spin flips. In Ref. 23, we have identified these correlated states as quantum Hall *ferrimagnets*.

A coherent superposition of two single-particle (SP) levels in a double well potential in the form of symmetrical and antisymmetrical states is a textbook example in quantum mechanics, which demonstrates a coherent charge oscillation between localized states of electron on two protons in H_2^+ molecules and a coherent oscillation between left handed and right handed amino acids.[24] Recent works based on this effect include a coherent control of Rabi oscillations of electron spin in quantum dots[7] and a macroscopic quantum resonance in the Cooper pair box problem in the mesoscopic superconducting grains.[25] The quantum Hall ferrimagnetic states or spin unbalanced phases[26,27] are also a direct manifestation of coherent quantum mechanical tunneling and interdot electronic correlations. These states can be described in terms of linear combinations of spin excitons localized in left and right dots, which in turn lead to coherent spin oscillations, e.g., spin counterpart of coherent charge oscillations in H_2^+ molecules.

The paper is organized as follows: in Sec. II, we review the Hamiltonian of electrons confined in the lateral gated quantum dots. In Sec. III, the computational methods of single-particle configuration interaction (SP-CI) and unrestricted Hartree–Fock configuration interaction (URHF-CI) are summarized. To differentiate the spin transitions of quantum dot molecules and two isolated dots with zero interdot interaction, we briefly present the spin phase diagram of single dots in Sec. IV. The microscopic picture of spin excitations in coupled quantum dots are discussed in Secs. V and VI. The interpretation of spin excitations in terms of electron-hole excitations allows us to attribute the excitations with total spin $S=1$ and $S=2$ as spin exciton and

biexciton.[28,29] Pairing of excitons and the formation of biexcitons due to strong interdot interaction is discussed. To elucidate the quantum Hall ferrimagnetic states, the real space representation of excitons is introduced. The paper is summarized in Sec. VII.

II. HAMILTONIAN

We describe electrons confined in quasi-two-dimensional quantum dots in a uniform perpendicular magnetic field by the effective mass Hamiltonian

$$H=\sum_{i=1}^{N}(T_i+E_{iZ})+\frac{e^2}{2\epsilon}\sum_{i\neq j}\frac{1}{|\vec{r}_i-\vec{r}_j|}, \tag{1}$$

where

$$T=\frac{1}{2m^*}\left(\frac{\hbar}{i}\vec{\nabla}+\frac{e}{c}A(\vec{r})\right)^2+V(x,y) \tag{2}$$

is the single electron Hamiltonian in a magnetic field. Here, $(\vec{r})=(x,y)$ describes electron position, $A(\vec{r})=\frac{1}{2}\vec{B}\times\vec{r}$ is the vector potential, B is the external magnetic field, and $V(\vec{r})$ is the quantum dot confining potential. m^* is the conduction-electron effective mass, e is the electron charge, and ϵ is the host semiconductor dielectric constant ($\epsilon=12.8$ in GaAs). $E_{iZ}=\frac{1}{2}g\mu_B\sigma_{iz}B$ is the Zeeman spin splitting, g is the host semiconductor g factor ($g=-0.44$ in GaAs), μ_B is the Bohr magneton, and σ is the Pauli matrix. In what follows, we present the numerical results in effective atomic unit (in GaAs effective Bohr radii $a_0^*=9.79$ nm and effective Rydberg Ry*$=5.93$ meV).

The single-particle eigenvalues (ϵ_i) and eigenvectors (φ_i) are calculated by discretizing T in real space and diagonalizing the resulting matrix using conjugate gradient algorithms.[20] The details of this calculation can be found in Ref. 33.

III. MANY-BODY SPECTRUM

To calculate the spectrum of interacting electrons, described by a Hamiltonian H in Eq. (1), we employ either the real space single-particle or unrestricted Hartree–Fock (URHF) states in configuration interaction techniques.[33] In the first SP-CI approach, single-particle levels are used to construct many-electron configurations, which are the basis of a configuration interaction (CI) Hamiltonian. By denoting the creation (annihilation) operators for electrons in a noninteracting SP state $|\alpha\sigma\rangle$ by $c_{\alpha\sigma}^{\dagger}$ ($c_{\alpha\sigma}$), the Hamiltonian of an interacting electron system in second quantization can be written as

$$H=\sum_{\alpha}\sum_{\sigma}\epsilon_{\alpha}c_{\alpha\sigma}^{\dagger}c_{\alpha\sigma}+\frac{1}{2}\sum_{\alpha\beta\gamma\mu}\sum_{\sigma\sigma'}V_{\alpha\sigma,\beta\sigma',\gamma\sigma',\mu\sigma}c_{\alpha\sigma}^{\dagger}c_{\beta\sigma'}^{\dagger}c_{\gamma\sigma'}c_{\mu\sigma}, \tag{3}$$

where the first term is the single-particle Hamiltonian, and $V_{\alpha\sigma,\beta\sigma',\gamma\sigma',\mu\sigma}=\int d\vec{r}\int d\vec{r}'\,\varphi_{\alpha\sigma}^{*}(\vec{r})\varphi_{\beta\sigma'}^{*}(\vec{r}')\frac{e^2}{\epsilon|\vec{r}-\vec{r}'|}\varphi_{\gamma\sigma'}(\vec{r}')\varphi_{\mu\sigma}(\vec{r})$ is the two-body Coulomb matrix element. In the configuration interaction method, the Hamiltonian of an interacting system is calculated on the basis of a finite number of many-electron configurations. The total number of configurations (or Slater determinants participating in CI calculation) is determined by

$$N_C=\left[\frac{N_s!}{N_{\uparrow}!(N_s-N_{\uparrow})!}\right]\left[\frac{N_s!}{N_{\downarrow}!(N_s-N_{\downarrow})!}\right]. \tag{4}$$

Here, N_s is the number of single-particle levels, and $N_{\uparrow}$ and $N_{\downarrow}$ are the number of spin up and spin down electrons. This Hamiltonian is either exactly diagonalized for small systems or low energy eigenvalues, and eigenstates are approximately extracted for a very large number of configurations.[33] With increasing number of single-particle levels N_s, the number of configurations N_C grows very fast, yet a large number is needed to accurately account for the direct and exchange interaction and electronic correlations. To improve the convergence of CI method, we incorporate direct and exchange contributions into the basis states by replacing SP states with states obtained by the URHF-CI. This implies expressing the new creation (annihilation) operators for URHF quasiparticles by $a_{i\sigma}^{\dagger}$ ($a_{i\sigma}$), with the index i representing the URHF orbit quantum numbers. The URHF basis can be expanded in a linear combination of SP states. In terms of SP creation (annihilation) operators, we write

$$a_{i\sigma}^{\dagger}=\sum_{\alpha=1}^{N_l}\lambda_{\alpha\sigma}^{(i)}c_{\alpha\sigma}^{\dagger}. \tag{5}$$

The transformation coefficients, $\lambda_{\alpha\sigma}^{(i)}$, satisfy the self-consistent Pople–Nesbet equations[20,30,31,33] as follows:

$$\sum_{\gamma=1}^{N_l}\left\{\epsilon_{\mu}\delta_{\gamma\mu}+\sum_{\alpha,\beta=1}^{N_l}\left(V_{\mu\alpha\beta\gamma}\sum_{\sigma'}\sum_{j=1}^{N_{\sigma'}}\lambda_{\alpha\sigma'}^{*(j)}\lambda_{\beta\sigma'}^{(j)}-V_{\mu\alpha\gamma\beta}\sum_{\sigma'}\sum_{j=1}^{N_{\sigma'}}\lambda_{\alpha\sigma'}^{*(j)}\lambda_{\beta\sigma'}^{(j)}\delta_{\sigma,\sigma'}\right)\right\}\lambda_{\gamma\sigma}^{(i)}=\epsilon_{i\sigma}^{HF}\lambda_{\mu\sigma}^{(i)}, \tag{6}$$

where $\epsilon_{i\sigma}^{HF}$ are the URHF eigenenergies. The N-lowest energy URHF levels form a Slater determinant occupied by Hartree–Fock (HF) quasielectrons, which corresponding to the HF ground state. The rest of the orbitals with higher energies are outside of the HF Slater determinant (unoccupied HF levels), contribute to electronic correlations, and can be used for CI calculation. The many-body Hamiltonian of the interacting system in the URHF basis can finally be written as

$$H=\sum_{\sigma}\sum_{ij}\langle i\sigma|T|j\sigma\rangle a_{i\sigma}^{\dagger}a_{j\sigma}+\frac{1}{2}\sum_{ijkl}\sum_{\sigma}\sum_{\sigma'}U_{i\sigma,j\sigma',k\sigma',l\sigma}a_{i\sigma}^{\dagger}a_{j\sigma'}^{\dagger}a_{k\sigma'}a_{l\sigma}, \tag{7}$$

where $U_{i\sigma,j\sigma',k\sigma',l\sigma}$ are the Coulomb matrix elements in the URHF basis. Here,

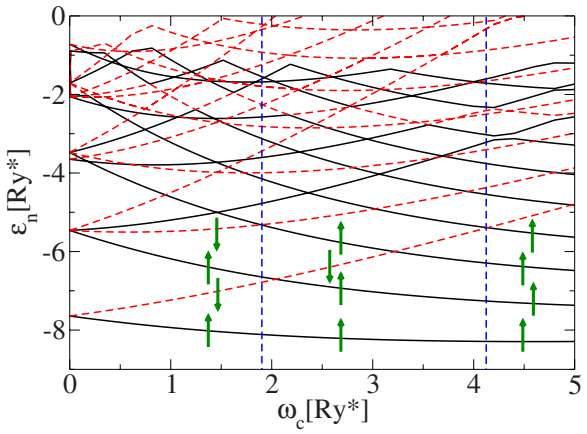

FIG. 1. (Color online) Single-particle spectrum as a function of cyclotron frequency ω_c for a Gaussian single dot with strength $V_0=-10$ Ry*, and $\Delta=2.5a_0^*$ in the presence of Zeeman splitting. Arrows represent spin of electrons. For illustration purposes, a very high Zeeman coupling $g=-9$ is used.

$$\langle i\sigma|T|j\sigma\rangle = \epsilon_{i\sigma}^{HF}\delta_{ij} - \langle i\sigma|U_H - U_X|j\sigma\rangle, \tag{8}$$

where U_H and U_X are the Hartree and exchange operators

$$\langle i\sigma|U_H|j\sigma\rangle = \sum_{\alpha\beta\mu\nu=1}^{N_l} V_{\alpha\mu\gamma\beta}\lambda_{\mu\sigma}^{*(i)}\lambda_{\gamma\sigma}^{(j)}\sum_{\sigma'}\sum_{k=1}^{N_{\sigma'}}\lambda_{\alpha\sigma'}^{*(k)}\lambda_{\beta\sigma'}^{(k)},$$

$$\langle i\sigma|U_X|j\sigma\rangle = \sum_{\alpha\beta\mu\nu=1}^{N_l} V_{\alpha\mu\beta\gamma}\lambda_{\alpha\sigma}^{*(i)}\lambda_{\beta\sigma}^{(j)}\sum_{k=1}^{N_\sigma}\lambda_{\mu\sigma}^{*(k)}\lambda_{\gamma\sigma}^{(k)}.$$

The resulting CI Hamiltonian matrix constructed on the basis of URHF configurations is either exactly diagonalized for small systems or low energy eigenvalues and eigenstates are approximately extracted for a very large number of configurations.[33] The details of the calculation and the convergence of the results as a function of the number of basis and configurations, and comparison between SP-CI and URHF-CI methods can be found in Ref. 33.

IV. SPIN TRANSITIONS IN SINGLE DOTS

We describe a single dot by an isotropic Gaussian confining potential $V(x,y)=V_0e^{-(x^2+y^2)/\Delta^2}$. The single-particle eigenenergies of such a quantum dot as a function of cyclotron frequency $\omega_c=eB/m^*$ are shown in Fig. 1.

States with spin up (down) are shown by bold (dashed) lines. For illustration, a very large g factor is introduced. We note in Fig. 1 that with an increasing magnetic field the energy of spin up (bold) levels decrease. These levels, and their spin down partners, correspond to the levels of the lowest Landau level (LLL). We now populate the lowest energy states with a number of electrons. From a previous work,[5] the minimum number of electrons that exhibit all nontrivial phenomena in the spin evolution of a single quantum dot is $N=4$. The $N=4$ configurations which minimize the kinetic energy are shown in Fig. 1. Due to the crossing of spin up and down levels, there are three different configurations: $S_z=0$, $S_z=1$, and $S_z=2$. These configurations illustrate increasing spin polarization of the electronic droplet with increasing magnetic field. With very small Zeeman energy, the increasing spin polarization in quantum dots is driven by electron-electron interactions. Hence, we turn off the Zeeman coupling and turn on electron-electron interactions.

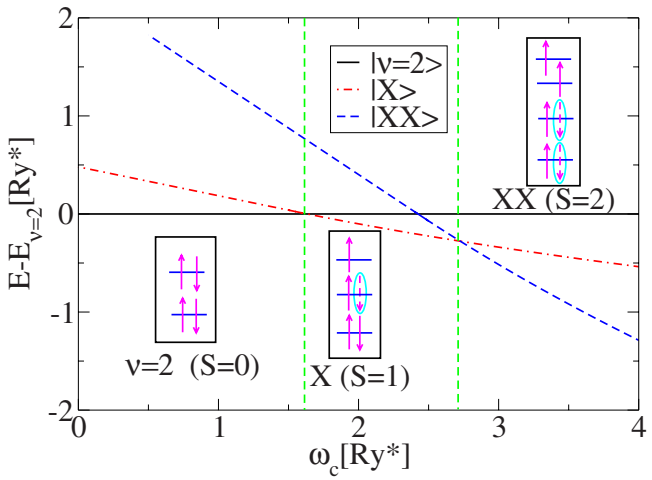

FIG. 2. (Color online) The energy of spin configurations shown in the boxes, $|\nu=2\rangle$, $|X\rangle$, and $|XX\rangle$ with total spins $S=0$, $S=1$, and $S=2$, using LLL orbitals, and $E_Z=0$. $E_{\nu=2}$ ($S=0$) is the reference of energy. The arrows surrounded by circles represent the holes.

We start with the lowest energy configuration built with SP LLL states, the $S_z=0$ spin singlet $\nu=2$ configuration $|\nu=2\rangle$. The spin excitations with $S=1$ and $S=2$ are constructed by removing electrons from occupied states and putting into unoccupied states, and can be described in terms of single exciton $|X\rangle$ and biexciton $|XX\rangle$ configurations, as shown in Fig. 2. By neglecting the mixing between configurations, we calculate the energy of each spin configuration. The result of this calculation is shown in Fig. 2. We chose the energy of the $S=0, \nu=2$ state ($E_{\nu=2}$) as the reference energy. As shown in Fig. 2, with increasing magnetic field even without Zeeman energy, both the first and second spin-flip transitions occur at $\omega_c=1.6$ and $\omega_c=2.75$ due to electron-electron interactions.

The effect of correlations on the evolution of spin of electrons in a single quantum dot obtained by the URHF-CI method is shown in Fig. 3. Here, the spin unpolarized ($S_z=0$) URHF states have been constructed out of $N_l=30$ SP states. $N_s=8$ HF levels have been taken to construct a CI Hamiltonian, which results in $N_C=784$ configurations. At zero magnetic field, we find $S=1$ triplet due to Hund's rule for electrons in a half-filled p shell. With increasing magnetic field, the single-particle energy gap opens up, which leads to a suppression of the $S=1$ triplet state and the formation of the $\nu=2$ ($S=0$) singlet state. The first spin-flip $S=1$ state appears at around $\omega=3$, followed by the second spin-flip spin polarized $S=2$ state at $\omega=4.5$. The flipping of the second spin is interrupted by a low-spin $S=0$ strongly correlated state. This state was previously identified with the formation of a spin singlet biexciton.[5] The first and second spin-flip states can be obtained for the noninteracting electrons and in Hartree–Fock approximation, while the formation of a spin

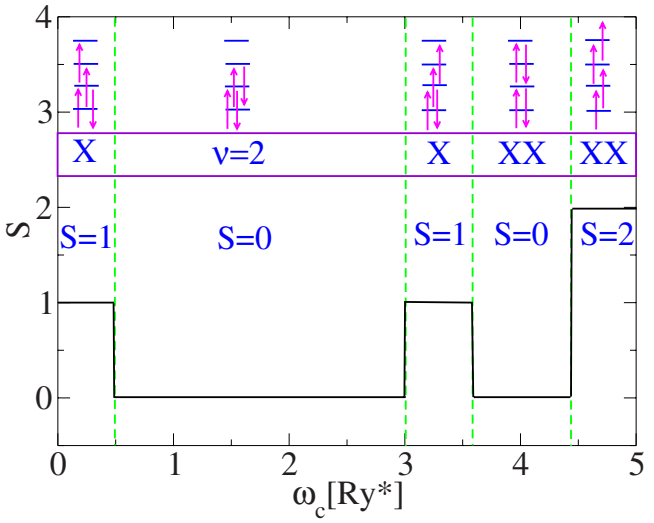

FIG. 3. (Color online) The spin evolution of the ground state of a single quantum dot as a function of magnetic field by using the URHF-CI method with $N_s=8$ HF levels, which correspond to $N_C=784$ configurations.

singlet biexciton is a result of electronic correlations in a quantum dot.

V. SPIN TRANSITIONS IN QUANTUM DOT MOLECULES

We now turn to study the spin transitions of laterally coupled quantum dots. We describe the molecule by electron (N_L,N_R) and ground state spin numbers (S_L,S_R) of isolated left (L) and right (R) dots. The spin phase diagram turns out to depend on electron numbers in each dot. Here, we will focus on molecules built out of identical dots with $N_L=N_R$. For a given number of electrons, the magnetic field will be used to tune their individual spin $S_L=S_R$. The goal will be to determine the total spin of the molecular system. The molecular coupling will be controlled by the height of the tunneling barrier. To illustrate the physics, we will discuss in detail the quantum dot molecule (4, 4) with four electrons each and contrast its properties with a single $N=4$ quantum dot discussed in a previous section.

A. One-electron spectrum of a quantum dot molecule

We parametrize quantum dot molecule potential in terms of a sum of three Gaussians $V(x,y)=V_L\exp[-\frac{(x+a)^2+y^2}{\Delta^2}]+V_R\exp[-\frac{(x-a)^2+y^2}{\Delta^2}]+V_p\exp[-\frac{x^2}{\Delta_{Px}^2}-\frac{y^2}{\Delta_{Py}^2}]$. Here, V_L and V_R describe the depths of the left and right quantum dot minima located at $x=-a$, $y=0$ and $x=+a$, $y=0$, and V_p is the central plunger gate potential the controls the tunneling barrier. The confining potential is parametrized as $V_L=V_R=-10$, $\Delta=2.5$, $a=2$, $\Delta_{Px}=0.3$, and $\Delta_{Py}=2.5$ in effective atomic units. The single-particle eigenvalues and eigenfunctions are numerically calculated by a discretization of the Schrödinger equation with the quantum dot molecule potential. The parameters of the confining potential considered in this work are chosen to represent weakly coupled quantum dots. At zero magnetic field, the SP levels of the electrons exhibit well separated s, p, and d electronic shells and, at high magnetic field, they form molecular shells of closely spaced pairs of bonding-antibonding orbitals. The half-filled molecular shells correspond to electron numbers $(N_L=2k-1,N_R=2k-1)$ and filled shells correspond to $(N_L=2k,N_R=2k)$ configurations (k is integer). The resulting single-particle spectrum as a function of magnetic field has been presented recently in Fig. 1 of Ref. 23. To understand and visualize the spectrum in a high magnetic field, we expand the confining potential in the vicinity of each minimum. This gives a parabolic potential $V(r)=m^*\omega_0^2r^2/2$ with the strength $\omega_0=2\sqrt{|V_0|/\Delta^2}$. The low energy spectrum of each dot corresponds to two harmonic oscillators with eigenenergies $\epsilon_{nm}=\omega_+(n+1/2)+\omega_-(m+1/2)$. Here, $\omega_\pm=\sqrt{\omega_0^2+\omega_c^2/4}\pm\omega_c/2$, ω_c is the cyclotron energy, and n, $m=0,1,2,\ldots$. With increasing magnetic field, the ω_- decreases to zero, while ω_+ approaches the cyclotron energy ω_c, and the states $|m,n\rangle$ evolve into the nth Landau level. In a high magnetic field, the corresponding wave functions admit a description in terms of localized LLL orbitals.[20] In this limit, linear combinations of the LLL orbitals m from left and right dots form molecular shells of closely spaced symmetric-antisymmetric pairs with eigenenergies approximately expressed as

$$\epsilon_{m\lambda\sigma}=\omega_-\left(m+\frac{1}{2}\right)-\lambda\frac{\Delta_m}{2}-\frac{1}{2}\sigma\gamma\omega_c. \tag{9}$$

Here, $E_Z=\gamma\omega_c$ is the Zeeman energy, $\sigma=+1(-1)$ corresponds to spin $\uparrow$ ($\downarrow$), $\gamma=m^*g$, and λ is the pseudospin index: the symmetric (antisymmetric) orbitals are labeled by $\lambda=+1(-1)$, which is the parity of the molecular orbitals. Δ_m is the symmetric-antisymmetric gap. The Zeeman coupling induces spin splitting with increasing magnetic field. This has been illustrated in Fig. 1 of Ref. 23. We now populate the quantum dot molecule with $N=8$ electrons. This is an example of electronic configurations corresponding to filled molecular shells. Figure 1 of Ref. 23 shows the evolution of the lowest energy states of noninteracting electrons, with the corresponding total spin S states separated by vertical lines. We find $S=0$, 2, and 4 phases with even S, which correspond to simultaneous spin flips in each isolated dot.

However, we also find odd S phases. The first odd spin state with $S=1$ occurs between magnetic fields corresponding to $\omega_{c1}^*\approx3.25$ and $\omega_{c2}^*\approx3.9$, where $\epsilon_{m=2,\sigma=\uparrow,\lambda=+1}=\epsilon_{m=1,\sigma=\downarrow,\lambda=-1}$ and $\epsilon_{m=2,\sigma=\uparrow,\lambda=-1}=\epsilon_{m=1,\sigma=\downarrow,\lambda=+1}$. The odd spin flip is related to the splitting of energy levels due to tunneling. By using single-particle eigenenergies given by Eq. (9), we find the first spin flip at the value of the magnetic field B_1 as follows:

$$\gamma\omega_c(1)=\omega_-(1)-\frac{\Delta_2(1)+\Delta_1(1)}{2}, \tag{10}$$

where the Zeeman energy is equal to the single dot level splitting minus the average symmetric-antisymmetric gap for the two levels involved. The second spin flip takes place at $\omega_c(2)$ such that

$$\gamma\omega_c(2) = \omega_-(2) + \frac{\Delta_2(2) + \Delta_1(2)}{2}. \tag{11}$$

Hence, the difference in the magnetic fields corresponding to first and second spin flips is a direct measure of the tunneling splitting as follows:

$$\gamma(\omega_c(2) - \omega_c(1)) = \frac{\Delta_2(2) + \Delta_1(2)}{2} + \frac{\Delta_2(1) + \Delta_1(1)}{2}. \tag{12}$$

From the spectrum of Fig. 1 of Ref. 23, we observe that the states with odd spins $S=1$ and $S=3$ are stable within a narrow range of magnetic fields due to spin-flip transitions among the electrons that occupy the levels with energy separation proportional to the interdot tunneling amplitude. This is in contrast to the first spin-flip transition in single dots (compare with Fig. 1), which is stable in a wide range of magnetic fields. For this reason, the existence of odd spin states in the spin phase diagram of quantum dot molecules can be interpreted as the measure of interdot interaction.

B. Many-electron quantum dot molecule spectrum

In this section, we present an analysis of spin transitions driven by electron-electron interaction. We focus on the tunnel coupled lowest Landau level orbitals m. By denoting the creation (annihilation) operators for an electron in a noninteracting SP state $|m\lambda\sigma\rangle$ by $c^\dagger_{m\lambda\sigma}(c_{m\lambda\sigma})$ (with σ as spin label), the Hamiltonian of an interacting system [Eq. (1)] can be written as

$$H = \sum_{m\lambda}\sum_{\sigma} \epsilon_{m\lambda\sigma} c^\dagger_{m\lambda\sigma} c_{m\lambda\sigma} + \frac{1}{2}\sum_{\{m,\lambda\}}\sum_{\sigma\sigma'} \langle m_1\lambda_1\sigma, m_2\lambda_2\sigma'|V|m_3\lambda_3\sigma', m_4\lambda_4\sigma\rangle \times c^\dagger_{m_1\lambda_1\sigma} c^\dagger_{m_2\lambda_2\sigma'} c_{m_3\lambda_3\sigma'} c_{m_4\lambda_4\sigma}. \tag{13}$$

The single-particle states of coupled quantum dot molecules in a magnetic field are labeled by the orbital quantum numbers m and the pseudospin index λ. The first term in Eq. (13) is the single-particle Hamiltonian, and $V_{\alpha\beta\mu\nu}$ is the two-body Coulomb matrix element. Here, $\{\alpha,\beta,\mu,\nu\}$ represent the states with quantum numbers (m,λ,σ). We now turn to the construction of the relevant configurations.

C. $S=0$, $\nu=2$ state

The $\nu=2$ state of a quantum dot molecule with N electrons and total spin $S=0$, shown in Fig. 4, is the product of electron creation operators

$$|\nu=2\rangle = \prod_{m=0}^{N/4-1}\prod_{\lambda=1,2}\prod_{\sigma=\uparrow,\downarrow} c^\dagger_{ms\sigma}|0\rangle. \tag{14}$$

The energy associated with this state

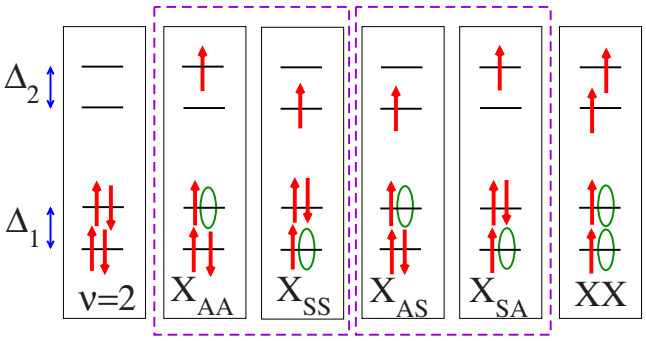

FIG. 4. (Color online) The basis of spin configurations in high magnetic fields. The first spin transition states $S=1$ identify with two independent sets: $\{X_{SS},X_{AA}\}$ and $\{X_{SA},X_{AS}\}$. In the former, the electron-hole transitions occur between the states with the same symmetry and, hence, they do not mix with the latter, which exhibits the process of electron-hole excitations between states with opposite parities.

$$E_{\nu=2} = \sum_{m=0}^{N/4-1}\sum_{\lambda=\pm1}\sum_{\sigma}[\epsilon_{m\lambda\sigma} + \Sigma(m,\lambda,\sigma)] \tag{15}$$

can be expressed in terms of self-energy $\Sigma(m,\lambda,\sigma)$ as follows:

$$\Sigma(m,\lambda,\sigma) = \sum_{m'=0}^{N/4-1}\sum_{\lambda'=\pm1}(2\langle m\lambda, m'\lambda'|V|m'\lambda', m\lambda\rangle - \langle m\lambda, m'\lambda'|V|m\lambda, m'\lambda'\rangle). \tag{16}$$

D. $S=1$ spin exciton

The $S=1$ spin-flip excitation is constructed by removing an electron from an occupied $\nu=2$ state and putting into an unoccupied state as follows:

$$|X_{j\to i}\rangle = c^\dagger_i c_j|\nu=2\rangle, \tag{17}$$

where $j\equiv(m,\lambda,\downarrow)$ and $i\equiv(m',\lambda',\uparrow)$. By denoting quasiparticle energy levels (electrons dressed by interaction) by $\varepsilon_i=\epsilon_i+\Sigma(i)$, the energy of one exciton is as follows:

$$\Delta E_{X_{j\to i}} = \varepsilon_i - \varepsilon_j - \langle i,j|V|j,i\rangle, \tag{18}$$

where $\Delta E_{X_{j\to i}} = E_{X_{j\to i}} - E_{\nu=2}$ is the energy of an exciton relative to the $\nu=2$ state energy. The last term in Eq. (18) is the electron-hole Coulomb attraction. The lowest energy states of the single exciton, which correspond to the first spin-flip state, are depicted in Fig. 4. We classify the single excitons based on their parity with respect to the parity of the $\nu=2$ state. A pair of states (X_{SS},X_{AA}) describes the transitions between pairs of levels with the same parity and so parity is conserved by these transitions. In contrast, spin-flip transitions represented by (X_{SA},X_{AS}) do not conserve parity as they describe transitions between pairs of levels with opposite parities. We identify (X_{SS},X_{AA}) and (X_{SA},X_{AS}) by their parity quantum numbers $\pi=+1$ and $\pi=-1$, respectively. It is important to note that Coulomb interactions do not mix excitons with different parities and the CI Hamiltonian con-

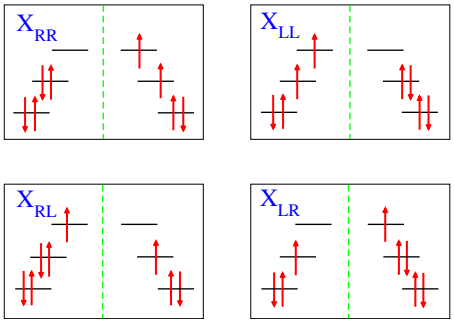

FIG. 5. (Color online) The lowest energy excitons in real space $|X_{RR}\rangle=|X_{(1,R,\downarrow)\to(2,R,\uparrow)}\rangle$, $|X_{LL}\rangle=|X_{(1,L,\downarrow)\to(2,L,\uparrow)}\rangle$, $|X_{RL}\rangle=|X_{(1,R,\downarrow)\to(2,L,\uparrow)}\rangle$, and $|X_{LR}\rangle=|X_{(1,L,\downarrow)\to(2,R,\uparrow)}\rangle$. The magnetic ordering of these states can be described by means of ferrimagnetic coupling $(S_L=0,S_R=1)$ for X_{RR} and $(S_L=1,S_R=0)$ for X_{LL}, and ferromagnetic coupling $(S_L=1/2,S_R=1/2)$ for X_{RL} and X_{LR}.

structed on the basis of spin excitons is block diagonal. These pairs of independent excitons are shown inside the boxes in Fig. 4.

In real space, single excitons can be expressed in terms of a linear combination of excitons localized in each dot. This basis is shown in Fig. 5. In each isolated dot, at a critical field, a transition from the $S=0$ singlet to the $S=1$ triplet state takes place. This configuration, which corresponds to X_{RR} and X_{LL} in Fig. 5, is equivalent to a localized electron-hole excitation in one dot in the presence of a background of electrons in the other dot. Because of the geometrical symmetry associated with the electron-hole excitation, the ground state of the system without external bias and interdot tunneling has double degeneracy: the state with $(S_L=0,S_R=1)$ has exactly the same energy as the state $(S_L=1,S_R=0)$. The many-body wave function of such a molecular state can be expressed as a linear combination of degenerate states $|S_L=0,S_R=1\rangle$ and $|S_L=1,S_R=0\rangle$. We identify these pairs of molecular states with quantum Hall ferrimagnets. For a range of magnetic field, these two states are separated from another pair of single excitations X_{LR} and X_{RL} with $(S_L=1/2,S_R=1/2)$ by an energy gap due to Coulomb interactions. In general, in the case of filled shells, molecular states with odd total spin S correspond to quantum Hall ferrimagnets. Our analysis of spin transitions in real space is presented in Sec. VI.

E. $S=2$ spin biexciton

With increasing magnetic fields, a higher polarized state with $S=2$ $(S_L=1,S_R=1)$, which is equivalent to a spin biexciton state, appears. A biexciton is constructed by removing a pair of electrons from occupied states and putting them into unoccupied states (see Fig. 4) as follows:

$$|XX_{j\to i,k\to l}\rangle = c_i^\dagger c_l^\dagger c_j c_k |\nu=2\rangle. \tag{19}$$

The energy of a biexciton can be decomposed into the energy of two single excitons plus their interaction,

$$\Delta E_{XX_{j\to i,k\to l}} = \Delta E_{X_{j\to i}} + \Delta E_{X_{k\to l}} + \delta V, \tag{20}$$

where $\Delta E_{X_{j\to i}}$ has been defined in Eq. (18). δV is the binding energy between two excitons, which accounts for the electron-electron, electron-hole, and hole-hole interactions, as follows:

$$\delta V = \langle l,i|V|i,l\rangle - \langle l,i|V|l,i\rangle - \langle l,j|V|j,l\rangle - \langle k,i|V|i,k\rangle + \langle j,k|V|k,j\rangle - \langle j,k|V|j,k\rangle. \tag{21}$$

F. First versus second spin flip in a quantum dot molecule

Unlike in a single quantum dot, the first spin-flip state $S=1$ is not an eigenstate of the coupled quantum dot Hamiltonian. There are two possible spin excitons for a given parity and they are coupled by Coulomb interactions. We use two distinct single exciton bases $\{X_{SS},X_{AA}\}$ and $\{X_{SA},X_{AS}\}$, labeled by parity $\pi=+1$ and $\pi=-1$, to construct the two 2×2 Hamiltonians. We denote by $\Delta E_{X_{SS}+X_{AA}}$, $\Delta E_{X_{SA}+X_{AS}}$ the lowest eigenenergies of these Hamiltonians.

Figure 6(a) shows the numerically calculated energies of odd parity spin excitons as a function of magnetic field. The energy $\Delta E_{X_{AS}}$ of spin exciton X_{AS} is positive for magnetic fields shown, but the energy $\Delta E_{X_{SA}}$ of spin exciton X_{SA} becomes negative at $\omega_c=3.8$, i.e., the X_{SA} spin-flip state becomes the lower energy state than the $\nu=2$, $S=0$ state. However, in stark contrast to a single quantum dot (Fig. 2), we find that the second spin-flip state XX becomes the ground state at a lower magnetic field $\omega_c=2.1$. Hence, unlike in a single quantum dot, we find a transition from a spin singlet $S=0$ state directly to a $S=2$ second spin-flip state. This is a transition corresponding to even total spin numbers, as if the two dots were simultaneously flipping their spins. However, correlations or mixing of the two spin excitons X_{AS} and X_{SA} lower the energy of the spin exciton. The energy $\Delta E_{X_{SA}+X_{AS}}$ of the correlated single spin state is significantly lower and is equal to both the energy ΔE_{XX} of the second spin-flip biexciton and of the $\nu=2$, $S=0$ state at $\omega_c=2.1$. At this value of the magnetic field, the energy of the biexciton and of the exciton are almost identical and, we might expect that for larger number of configurations, correlations will stabilize the single spin-flip exciton even further. The effect of correlations on the even parity excitons X_{AA} and X_{SS} is shown in Fig. 6(b). We see that a mixing of the two even parity excitons lowers the energy $\Delta E_{X_{SS}+X_{AA}}$ of the correlated single spin state. This energy is equal to both the energy ΔE_{XX} of the second spin-flip biexciton and of the $\nu=2,S=0$ state at $\omega_c=2.1$. By a comparison with Fig. 6(a), we see that the value of $\omega_c=2.1$ also corresponds to the change in parity of the single spin exciton $S=1$ state.

As illustrated in Fig. 6, with a mixing of single exciton configurations, the energy of a quantum dot molecule exhibits a fourfold degeneracy at ω_{c1}^*, where $S=0$ and $S=2$ and two different parity $S=1$ states become the lowest energy states. The $S=1$ states show stability in a narrow range of magnetic field, within the accuracy of our numerical results. With a further increase of magnetic field, single excitons

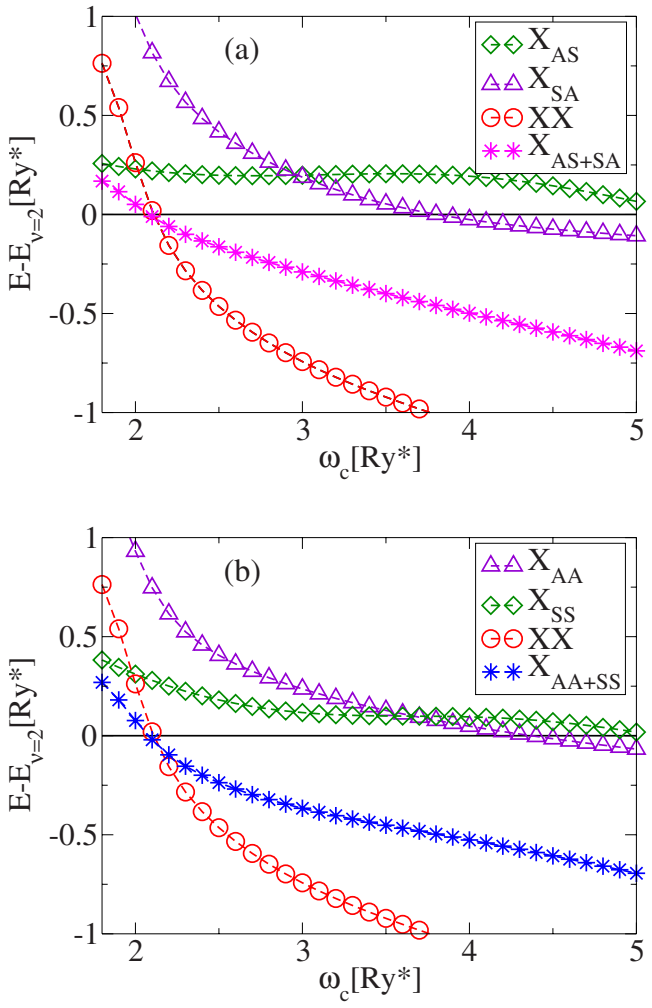

FIG. 6. (Color online) (a) The energies of two single spin excitons X_{SA} and X_{AS} with odd parity, the energy of the odd parity correlated exciton X_{SA+AS}, and the energy of the spin biexciton $S=2$ state as a function of magnetic field. All energies are measured from the energy of the $\nu=2$, $S=0$ state. (b) The energies of two single spin excitons X_{SS} and X_{AA} with even parity, the energy of the even parity correlated exciton X_{SS+AA}, and the energy of the spin biexciton $S=2$ state as a function of magnetic field. All energies are measured from the energy of the $\nu=2$, $S=0$ state.

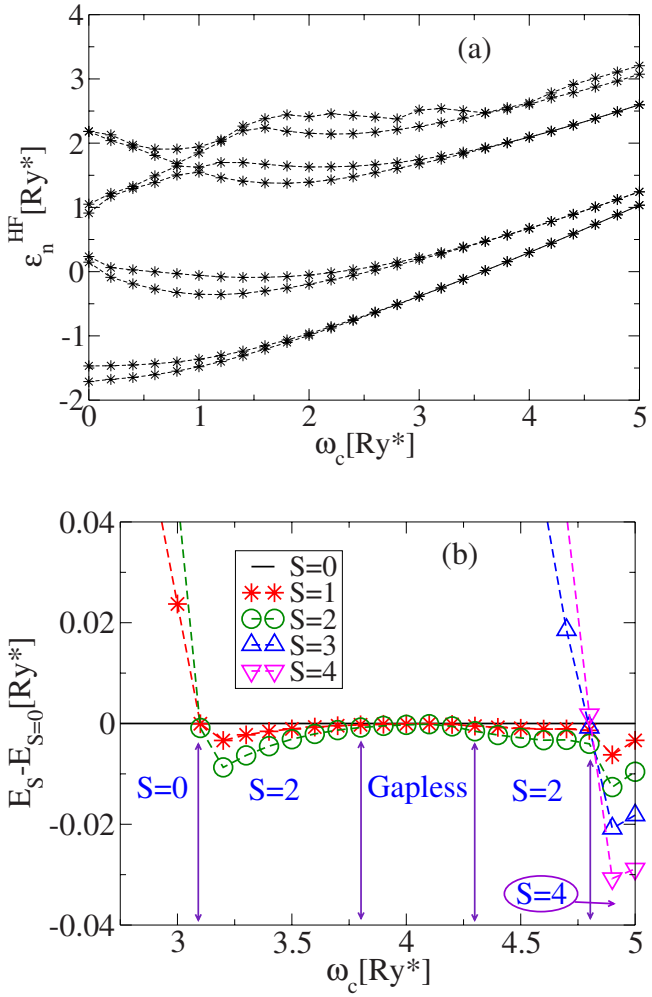

FIG. 7. (Color online) (a) URHF energies vs cyclotron energy for $N=8$ electrons with $S_z=0$. (b) Evolution of lowest energies for $S=0$, 1, and 2 states calculated by the URHF-CI method. The energies are measured from the energy of the $S=0$ state.

condense into pairs of excitons forming biexcitons. The existence of single, odd, spin excitons is hence a signature of electronic correlations. These states do not exist at the Hartree–Fock level.

To support the assertion that correlations are responsible for the existence of odd spin excitons, we employ the URHF-CI calculation. From the solution of the Pople–Nesbet equations, we obtain HF eigenenergies, shown in Fig. 7(a), for $N=8$ electrons with $S_z=0$, as a function of the magnetic field. The HF wave functions are used as a basis in the HF-CI calculation of the ground state. We employ $N_s=8$ HF basis states (equivalent to $N_C=4900$ configurations) to calculate the total spin of electrons in a quantum dot molecule as a function of the magnetic field. From this calculation, we find that the $S=0$, $S=1$, and $S=2$ states are almost degenerate at $\omega_{c1}^*=3.1$. The prediction of URHF-CI is in qualitative agreement with an effective SP-CI model, which is presented above. The direct, exchange, and correlation energies calculated by URHF-CI shift the transition point to higher magnetic fields.

With increasing magnetic field, we find that the gap between different total spin states tends to vanish. This gapless phase is seen in Figs. (7) and (8) in the vicinity of $\omega_c=4$. This phase is followed by the $S=2$, $S=3$, and $S=4$ states. The latter state corresponds to a fully spin polarized $\nu=1$ droplet.

Let us now summarize the similarities and differences in the evolution of the total spin of two isolated dots and a quantum dot molecule. Figure 8(a) shows the evolution of total spin with increasing magnetic field for two noninteracting $N=4$ quantum dots and for a $N=8$ quantum dot molecule. Figure 8(b) shows the energy gap of the molecule as a function of magnetic field. The noninteracting quantum dot spin evolution is obtained by adding the results from two isolated dots, with each dot evolving with the magnetic field according to Fig. 3. We find that the effect of interdot interaction is to renormalize the magnetic fields at which spin

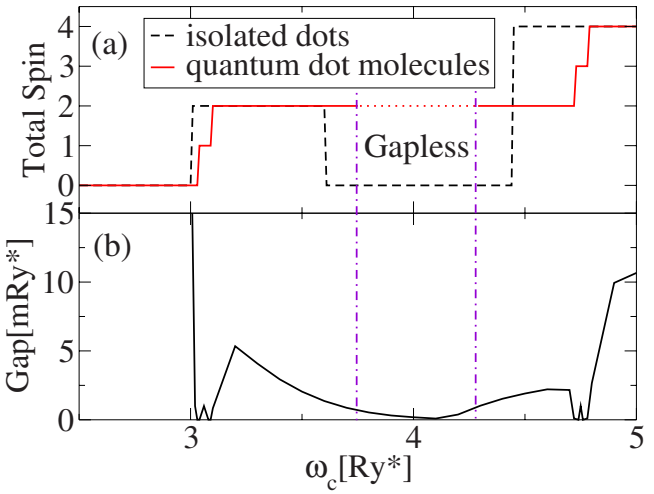

FIG. 8. (Color online) (a) The evolution of spin of the $N=8$ electron quantum dot molecules as a function of magnetic field for $g=0$ and $V_p=7$ (solid line). For comparison, the spin evolution of two isolated dots is shown (dashed line). The width of odd spin plateaux has been artificially enlarged to be visible to the eyes. The vertical dashed line (purple color online) tends to qualitatively show a range of ω_c in which the gap vanishes. The horizontal dashed line (red color) shows the corresponding spin one state with zero gap. (b) The evolution of the energy gap of the quantum dot molecules as a function of magnetic field.

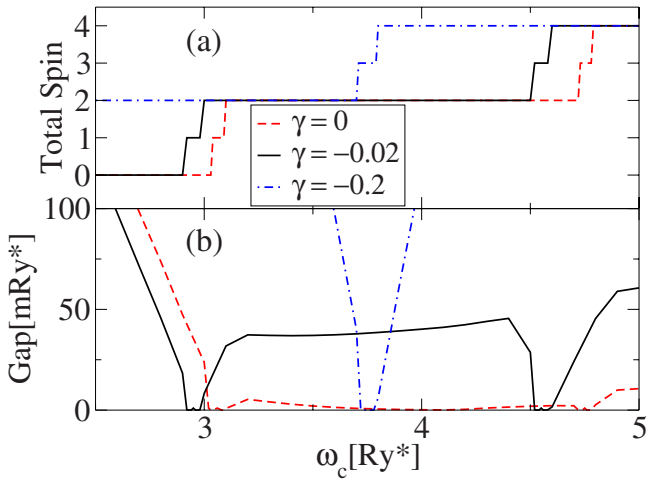

FIG. 9. (Color online) The effect of increasing the Zeeman energy on the (a) evolution of spin and (b) evolution of energy gap of the $N=8$ electron quantum dot molecules as a function of magnetic field. The width of $g=0$ odd spin plateaux have been artificially enlarged to be visible to the eyes.

transitions take place and, more importantly, to lead to the appearance of odd spin states $S=1$ and $S=3$. While the existence of odd spin states is most striking, the presence of spin polarized phases is also nontrivial. The fact that spins of electrons on two quantum dots align demonstrates the existence of ferromagnetic dot-dot coupling. In the case of antiferromagnetic coupling, there would have been no net spin even though each dot has a finite spin. We will show in Sec. VI that such an antiferromagnetic coupling exists in the $N=8$ molecule at low magnetic fields.

Finally, following the gap in Fig. 8(b), we find the existence of low spin "gapless" states, which are the molecular analogs of spin singlet biexcitons. Hence, Fig. 8 shows that electronic interdot correlations stabilize the odd spin phases, but their stability range is very narrow. As shown in Sec. V A, without electron-electron interactions, the competition between quantum mechanical tunneling and Zeeman energy was responsible for the existence of odd spin phases. The effect of a finite Zeeman energy is similar in an interacting system. Figure 9 shows the effect of increasing the Zeeman energy on the evolution of spin and energy gap of the $N=8$ electron quantum dot molecules as a function of magnetic field. All parameters are the same as in Fig. 8. We see that increasing the Zeeman energy renormalizes the magnetic field value of spin flips and, more importantly, stabilizes the odd spin phases. From the evolution of the energy gap shown in Fig. 9(b), we also see the vanishing of the low spin depolarized phase in the vicinity of $\omega_c=4$ and the stabilization of the spin polarized $S=2$ phase. The Zeeman energy depends on the g factor. For GaAs, the g factor is $g_{\mathrm{GaAs}}=-0.44$, while for InAs and InSb, the g factors are $g_{\mathrm{InAs}}=-14$ and $g_{\mathrm{InSb}}=-50$.[8–13] Hence, by adding In, one can hope to tune the g factor of quantum dot molecules.

To conclude our analysis of the $N=8$ electron quantum dot molecule, we discuss the effect of asymmetry between the two dots. While for molecules built out of two atoms each component is identical, quantum dots are defined by gates or etching and one must understand the effect of differences between the two dots on the stability diagram.[32] In Fig. 10, we show the evolution of spin and energy gap of the $N=8$ electron quantum dot molecules as a function of magnetic field. The two dots are different, with the confining potential of the left dot $V_L=-10$ unchanged but the potential of the right dot detuned by 1 Ry to $V_R=-11$. As anticipated, the effect of detuning results in an increased stability of the odd spin-flip state $S=1$.

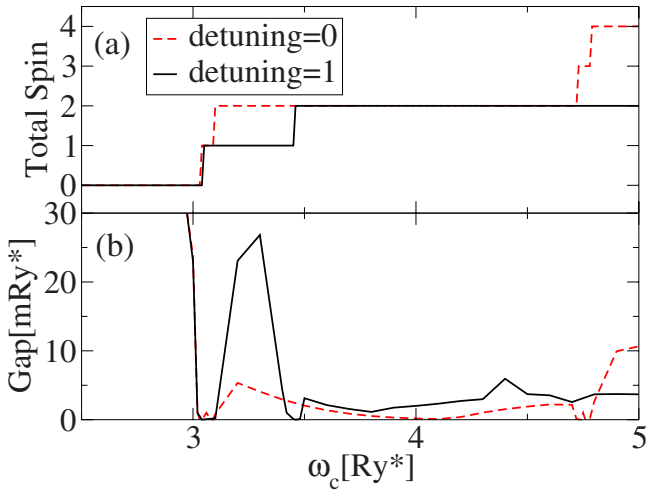

FIG. 10. (Color online) The effect of detuning, i.e., difference in confining potential between left dot V_L and right dot V_R, on the (a) evolution of spin and (b) evolution of the energy gap of the $N=8$ electron quantum dot molecules as a function of magnetic field.

VI. REAL SPACE ANALYSIS OF SPIN TRANSITIONS IN QUANTUM DOT MOLECULES

In this section, we describe the analysis of spin transitions in real space. Equation (13) describes the Hamiltonian of an interacting system in a second quantization in a noninteracting SP state $|m\lambda\sigma\rangle$. The single-particle states of coupled quantum dot molecules in a magnetic field are labeled by the single dot orbital quantum numbers m and the pseudospin index λ. The symmetric (antisymmetric) orbitals are labeled by $\lambda=1(-1)$, which is the parity of the orbitals in two symmetric dots. m represents the combined Landau level and angular momentum quantum numbers, $m\equiv(n,l)$. The first term in Eq. (13) is the single-particle Hamiltonian, and $V_{\alpha\sigma,\beta\sigma',\mu\sigma',\nu\sigma}=\int d\vec{r}\int d\vec{r}'\,\tilde{\varphi}^*_{\alpha\sigma}(\vec{r})\tilde{\varphi}^*_{\beta\sigma'}(\vec{r}')\frac{e^2}{\epsilon|\vec{r}-\vec{r}'|}\tilde{\varphi}_{\mu\sigma'}(\vec{r}')\tilde{\varphi}_{\nu\sigma}(\vec{r})$ is the two-body Coulomb matrix element. Here, $\{\alpha,\beta,\mu,\nu\}$ represent the states with orbital quantum numbers (m,λ).

By alternatively denoting the creation (annihilation) operators for an electron in a noninteracting localized SP state $|ms\sigma\rangle$ by $d^\dagger_{ms\sigma}$ ($d_{ms\sigma}$), the Hamiltonian of an interacting system in second quantization can be written as

$$H=\sum_{ms}\sum_{\sigma}\tilde{\epsilon}_{ms}d^\dagger_{ms\sigma}d_{ms\sigma}+\sum_{m\sigma}t_m\sum_{s_1s_2}(1-\delta_{s_1s_2})d^\dagger_{ms_1\sigma}d_{ms_2\sigma}+\frac{1}{2}\sum_{\{m,s\}}\sum_{\sigma\sigma'}\langle m_1s_1\sigma,m_2s_2\sigma'|V|m_3s_3\sigma',m_4s_4\sigma\rangle\times d^\dagger_{m_1s_1\sigma}d^\dagger_{m_2s_2\sigma'}d_{m_3s_3\sigma'}d_{m_4s_4\sigma}. \quad (22)$$

Here, $s=1$ (2) are pseudospin labels of an electron localized in the left (right) dot. The relation between Eqs. (13) and (22) can be established by a rotation in pseudospin space $c^\dagger_{m\lambda\sigma}=\frac{1}{\sqrt{2}}\Sigma_{s=1}^2\lambda^{s-1}d^\dagger_{ms\sigma}$. We find $\tilde{\epsilon}_{ms}=(\epsilon_{m,\lambda=1}+\epsilon_{m,\lambda=-1})/2$, $t_m=(\epsilon_{m,\lambda=1}-\epsilon_{m,\lambda=-1})/2$, and

$$\langle m_1s_1\sigma,m_2s_2\sigma'|V|m_3s_3\sigma',m_4s_4\sigma\rangle=\frac{1}{4}\sum_{\lambda}\lambda_1^{s_1-1}\lambda_2^{s_2-1}\lambda_3^{s_3-1}\lambda_4^{s_4-1}\times\langle m_1\lambda_1\sigma,m_2\lambda_2\sigma'|V|m_3\lambda_3\sigma',m_4\lambda_4\sigma\rangle. \quad (23)$$

A. $S=0$ ground state

The $\nu=2$ state of a quantum dot molecule with N electrons and total spin $S=0$ is the product of spin polarized localized electrons as follows:

$$|\nu=2\rangle=\prod_{m=0}^{N/4-1}\prod_{s=1,2}\prod_{\sigma=\uparrow,\downarrow}d^\dagger_{ms\sigma}|0\rangle. \quad (24)$$

The energy associated with this state is as follows:

$$E_{\nu=2}=\sum_{m=0}^{N/4-1}\sum_{s=1}^{2}[2\tilde{\epsilon}_{ms}+\Sigma(m,s)], \quad (25)$$

where $\Sigma(m,s)$ is the electron self-energy,

$$\Sigma(m,s)=\sum_{m'=0}^{N/4-1}\sum_{s'=1}^{2}(2\langle ms,m's'|V|m's',ms\rangle-\langle ms,m's'|V|ms,m's'\rangle). \quad (26)$$

B. $S=1$ exciton

In each isolated dot, at a critical field, and driven by electron Coulomb interaction, accompanied with increasing electron kinetic energy, a transition from $S=0$ singlet to $S=1$ triplet is seen. The cost in kinetic energy is lowered if localized electrons in one dot flip the spin ($S_L=1$), while the other electrons in the second dot occupy the lowest energy single-particle states to form a spin singlet droplet ($S_R=0$). This configuration, which corresponds to X_{RR} (or X_{LL}) in Fig. 5, is equivalent to a localized electron-hole excitation in one dot in the presence of the background of electrons in the other dot. Because of the geometrical symmetry associated with the electron-hole excitation, the ground state of the system (without any external bias and interdot tunneling) has double degeneracy: the state with $(S_L=0,S_R=1)$ has exactly the same energy as the state $(S_L=1,S_R=0)$. The many-body wave function of such a molecular state can be expressed as a linear combination of degenerate states $|S_L=0,S_R=1\rangle$ and $|S_L=1,S_R=0\rangle$. We identify these pair of excitations as quantum Hall ferrimagnets. For a range of magnetic fields, these two states are separated from another pair of single excitations X_{LR} and X_{RL} with $(S_L=1/2,S_R=1/2)$ by an energy gap (because of Coulomb interaction). In general, in the case of filled shells, molecular states with $S=$(odd) form quantum Hall ferrimagnetism, which may give rise to an experimentally observable ferrimagnetic resonance.

An excitonic state is constructed by removing an electron from an occupied state and putting it into an unoccupied state,

$$|X_{j\to i}\rangle=d^\dagger_i d_j|\nu=2\rangle, \quad (27)$$

where $j\equiv(m,s,\downarrow)$ and $i\equiv(m',s',\uparrow)$. The lowest energy basis of the single exciton (first spin-flip state) are depicted in Fig. 5. By labeling the direct and indirect spin-flip transitions (with ferrimagnetic and ferromagnetic spin ordering) by $\{X_{RR},X_{LL}\}$ and $\{X_{LR},X_{RL}\}$ and by using their symmetries, we find that the direct (indirect) states are twofold degenerate, $E_{X_{RR}}=E_{X_{LL}}$ ($E_{X_{LR}}=E_{X_{RL}}$). Here, the subscripts are defined as $RR\equiv(1,R,\downarrow)\to(2,R,\uparrow)$, $LL\equiv(1,L,\downarrow)\to(2,L,\uparrow)$, $RL\equiv(1,R,\downarrow)\to(2,L,\uparrow)$, and $LR\equiv(1,L,\downarrow)\to(2,R,\uparrow)$. Note that in a noninteracting system, the basis is fourfold degenerate, $E_{X_{RR}}=E_{X_{LL}}=E_{X_{LR}}=E_{X_{RL}}$.

By denoting quasiparticle energy levels (electrons dressed by interaction) by $\varepsilon_i=\tilde{\epsilon}_i+\Sigma(i)$, the energy of one exciton holds,

$$E_{X_{j\to i}}=E_{\nu=2}+\varepsilon_i-\varepsilon_j-\langle i,j|V|j,i\rangle. \quad (28)$$

The last term is the electron-hole Coulomb interaction. On the basis of single excitonic states, the Hamiltonian of the quantum dot molecules can be expressed as

$$H^{\text{eff}}_{4\times4} = T^{\text{eff}}_{4\times4} + V^{\text{eff}}_{4\times4}, \tag{29}$$

where

$$T^{\text{eff}}_{4\times4} = \begin{pmatrix} E_{X_{RR}} & 0 & +t_1 & -t_2 \\ 0 & E_{X_{LL}} & -t_2 & +t_1 \\ +t_1 & -t_2 & E_{X_{LR}} & 0 \\ -t_2 & +t_1 & 0 & E_{X_{RL}} \end{pmatrix} \tag{30}$$

is the noninteracting part and

$$V^{\text{eff}}_{4\times4} = \begin{pmatrix} 0 & V_{RRLL} & V_{RRLR} & V_{RRRL} \\ V^*_{RRLL} & 0 & V_{LLLR} & V_{LLRL} \\ V^*_{RRLR} & V^*_{LLLR} & 0 & V_{LRRL} \\ V^*_{RRRL} & V^*_{LLRL} & V^*_{LRRL} & 0 \end{pmatrix} \tag{31}$$

is the Coulomb interaction between the single excitonic states.

Note that the pair of states X_{RR} and X_{LL} are not coupled by the single tunneling term, because the scattering process between X_{RR} and X_{LL} requires the simultaneous exchange of two particles. For that reason, this process is second order in tunneling. The same is true for the states X_{LR} and X_{RL}.

C. $S=2$ biexciton

With increasing magnetic fields, a higher polarized state with $S=2$ ($S_L=1, S_R=1$), which is equivalent to a biexcitonic state, tends to appear as a ground state. A biexciton is constructed by removing a pair of electrons from occupied states and putting than into unoccupied states,

$$|X_{j\to i,k\to l}\rangle = d^\dagger_i d^\dagger_l d_j d_k |\nu=2\rangle. \tag{32}$$

The energy of a biexcitonic state can be decomposed into the energy of two single excitons plus their interaction,

$$\Delta E_{XX_{j\to i,k\to l}} = \Delta E_{X_{j\to i}} + \Delta E_{X_{k\to l}} + \delta V. \tag{33}$$

δV is the binding energy between two excitons, which accounts for the electron-electron, electron-hole, and hole-hole interactions, as follows:

$$\begin{aligned}\delta V = &\langle l,i|V|i,l\rangle - \langle l,i|V|l,i\rangle - \langle l,j|V|j,l\rangle - \langle k,i|V|i,k\rangle \\ &+ \langle j,k|V|k,j\rangle - \langle j,k|V|j,k\rangle.\end{aligned} \tag{34}$$

In the quantum dot molecule considered in this study, we find $\delta V<0$ for large magnetic fields, i.e., two isolated excitons favor to pair and form a biexcitonic state, where the energy of a biexciton is lower than the energy of two isolated single excitons.

D. Excitonic condensation: A single-particle configuration interaction effective model

The eigenvalues of $T^{\text{eff}}_{4\times4}$ follow $E_{AS}<E_{SS}<E_{AA}<E_{SA}$ (as $t_2>t_1$). The corresponding eigenstates are $|X_{AS}\rangle$, $|X_{SS}\rangle$, $|X_{AA}\rangle$, and $|X_{SA}\rangle$, as shown in Fig. 4. Note that in noninteracting electrons, $\Delta E^0_X = E^0_X - E_{\nu=2} > 0$, where $E^0_X = E_{X_{RR}} = E_{X_{LL}} = E_{X_{RL}} = E_{X_{LR}}$. By simplifying the Coulomb interaction among electrons as $V_{ijkl} \to V_0 > 0$, we can analytically calculate the self-energy and the ground state energy of the $S=0$ state as $\Sigma = NV_0/2$ and $E_{\nu=2} = E^0_{\nu=2} + (N/2)^2 V_0$. The latter is the energy of a single exciton from the ground state energy. We can also calculate the energy of a single exciton $\Delta E_{X_{j\to i}} = \epsilon_i - \epsilon_j - V_0 < \Delta E^0_X$ and the energy of the biexciton $\Delta E_{XX} = 2\Delta E_X - 2V_0$, where $\Delta E_X \equiv \Delta E_{X_{RR}} = \Delta E_{X_{LL}}$ and $\delta V = -2V_0 < 0$. The energy difference between a biexciton and a single exciton follows $\Delta E_{XX} - \Delta E_X = \Delta E_X - 2V_0$. In the limit of a strong Coulomb interaction (large magnetic fields), we find $\epsilon_i - \epsilon_j < 3V_0$ and $E_{XX} < E_X$.

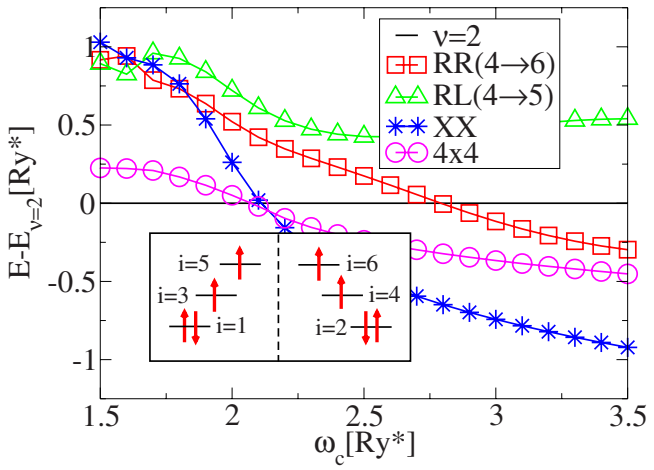

FIG. 11. (Color online) The energies of spin excitons with respect to $\nu=2$, $S=0$ state as a function of magnetic field. E^{eff}_1 is the lowest eigenenergy of the effective Hamiltonian $H^{\text{eff}}_{4\times4}$. The inset illustrates the energy levels of single-particle localized states.

The energy of interacting electrons with two distinct single excitons corresponding to the direct and indirect first spin-flip transitions, X_{RR} and X_{LR}, the lowest energy eigenvalue of $H^{\text{eff}}_{4\times4}$, and the energy of a biexciton ($S=2$), calculated from the ground state energy with $S=0$, are shown in Fig. 6.

Predicted by single configuration SP-CI, the direct spin-flip transition takes place at $\hbar\omega^*_{c1} \approx 2.8$, where $E_{X_{RR}} < E_{\nu=2}$, as shown in Fig. 11. Within this range of magnetic fields, the energy of a biexciton is lower than the energy of a single exciton due to strong Coulomb interaction, where at $\hbar\omega^*_{c2} \approx 2.1$, a transition to $S=2$ state is seen due to pairing of single spin excitons and, thus, single excitons condensate into a pair of excitons (biexcitons). However, because of a strong mixing between the single excitonic states, electron correlations significantly improve the energy of $S=1$ state such that it brings the first spin-flip transition point to $\hbar\omega^*_{c1} \approx \hbar\omega^*_{c2}$, where three states with $S=0$, $S=1$, and $S=2$ appeared to be almost degenerate. The Zeeman coupling removed such degeneracy. As a result, the $S=1$ state tends to become stable in a narrow range of magnetic field.

VII. CONCLUSION

In conclusion, we have presented the magnetic field driven spin transitions of quantum dot artificial molecules with $N=8$ as a function of external magnetic field, Zeeman energy, and detuning, using the Hartree–Fock configuration interaction method. The magnetic field allows the tuning of the total spin of electrons in each artificial atom. Quantum mechanical tunneling and electron-electron interactions couple spins of each artificial atom and result in ferromagnetic, antiferromagnetic, and ferrimagnetic states of quantum dot artificial molecules tunable by the magnetic field and barrier potential.

ACKNOWLEDGMENTS

The authors acknowledge the support by the NRC High Performance Computing project and by the Canadian Institute for Advanced Research.

[1] W. G. van der Wiel, S. De Franceschi, J. M. Elzerman, T. Fujisawa, S. Tarucha, and L. P. Kouwenhoven, Rev. Mod. Phys. **75**, 1 (2003).
[2] M. Ciorga, A. Wensauer, M. Pioro-Ladriere, M. Korkusinski, J. Kyriakidis, A. S. Sachrajda, and P. Hawrylak, Phys. Rev. Lett. **88**, 256804 (2002).
[3] M. Pioro-Ladriere, M. Ciorga, J. Lapointe, P. Zawadzki, M. Korkusinski, P. Hawrylak, and A. S. Sachrajda, Phys. Rev. Lett. **91**, 026803 (2003).
[4] J. R. Petta, A. C. Johnson, C. M. Marcus, M. P. Hanson, and A. C. Gossard, Phys. Rev. Lett. **93**, 186802 (2004).
[5] M. Korkusinski, P. Hawrylak, M. Ciorga, M. Pioro-Ladriere, and A. S. Sachrajda, Phys. Rev. Lett. **93**, 206806 (2004).
[6] J. R. Petta, A. C. Johnson, J. M. Taylor, E. A. Laird, A. Yacoby, M. D. Lukin, C. M. Marcus, M. P. Hanson, and A. C. Gossard, Science **309**, 2180 (2005).
[7] F. H. L. Koppens, C. Buizert, K. J. Tielrooij, I. T. Vink, K. C. Nowack, T. Meunier, L. P. Kouwenhoven, and L. M. K. Vandersypen, Nature (London) **442**, 766 (2006).
[8] S. Sasaki, D. G. Austing, and S. Tarucha, Physica B **256**, 157 (1998).
[9] L. P. Kouwenhoven, D. G. Austing, and S. Tarucha, Rep. Prog. Phys. **64**, 701 (2001).
[10] R. Hanson, B. Witkamp, L. M. K. Vandersypen, L. H. Willems van Beveren, J. M. Elzerman, and L. P. Kouwenhoven, Phys. Rev. Lett. **91**, 196802 (2003).
[11] D. G. Austing, S. Tarucha, H. Tamura, K. Muraki, F. Ancilotto, M. Barranco, A. Emperador, R. Mayol, and M. Pi, Phys. Rev. B **70**, 045324 (2004).
[12] B. D. McCombe and R. J. Wagner, Phys. Rev. B **4**, 1285 (1971).
[13] I. Žutić, J. Fabian, and S. Das Sarma, Rev. Mod. Phys. **76**, 323 (2004).
[14] J. J. Palacios and P. Hawrylak, Phys. Rev. B **51**, 1769 (1995).
[15] A. Galindo and M. A. Martin-Delgado, Rev. Mod. Phys. **74**, 347 (2002).
[16] J. A. Brum and P. Hawrylak, Superlattices Microstruct. **22**, 431 (1997).
[17] D. Loss and D. P. DiVincenzo, Phys. Rev. A **57**, 120 (1998); G. Burkard, D. Loss, and D. P. DiVincenzo, Phys. Rev. B **59**, 2070 (1999).
[18] Xuedong Hu and S. Das Sarma, Phys. Rev. A **64**, 042312 (2001); X. Hu and S. Das Sarma, *ibid.* **61**, 062301 (2000).
[19] J. Kolehmainen, S. M. Reimann, M. Koskinen, and M. Manninen, Eur. Phys. J. B **13**, 731 (2000).
[20] Ramin M. Abolfath, W. Dybalski, and Pawel Hawrylak, Phys. Rev. B **73**, 075314 (2006).
[21] L. Martin-Moreno, L. Brey, and C. Tejedor, Phys. Rev. B **62**, R10633 (2000); David Sanchez, L. Brey, and Gloria Platero, *ibid.* **64**, 235304 (2001).
[22] S. M. Girvin and A. H. MacDonald, in *Perspectives in Quantum Hall Effects: Novel Quantum Liquids in Low-Dimensional Semiconductor Structures*, edited by S. Das Sarma and A. Pinczuk (Wiley, New York, 1997).
[23] Ramin M. Abolfath and Pawel Hawrylak, Phys. Rev. Lett. **97**, 186802 (2006).
[24] J. J. Sakurai, *Modern Quantum Mechanics*, 2nd ed. (Addison-Wesley, Reading, MA, 1994).
[25] Y. Nakamura, C. D. Chen, and J. S. Tsai, Phys. Rev. Lett. **79**, 2328 (1997); Y. Nakamura, Yu. A. Pashkin, and J. S. Tsai, Nature (London) **398**, 786 (1999).
[26] James Smart, *Effective Field Theories of Magnetism* (Saunders, Philadelphia, 1966).
[27] S. Yamamoto, Phys. Rev. B **69**, 064426 (2004); S. Yamamoto, T. Fukui, K. Maisinger, and U. Schollwck, J. Phys.: Condens. Matter **10**, 11033 (1998); M. Abolfath, H. Hamidian, and A. Langari, arXiv:cond-mat/9901063 (unpublished), and references therein.
[28] Andreas Wensauer, Marek Korkusinski, and Pawel Hawrylak, Phys. Rev. B **67**, 035325 (2003).
[29] V. W. Scarola and S. Das Sarma, Phys. Rev. A **71**, 032340 (2005).
[30] A. Szabo and N. S. Ostlund, *Modern Quantum Chemistry* (McGraw-Hill, New York, 1989).
[31] Constantine Yannouleas and Uzi Landman, Phys. Rev. B **68**, 035325 (2003); **68**, 035325 (2003); C. Yannouleas and U. Landman, J. Phys.: Condens. Matter **14**, L591 (2002); Int. J. Quantum Chem. **90**, 699 (2002).
[32] M. Pioro-Ladriere, R. M. Abolfath, P. Zawadzki, J. Lapointe, S. A. Studenikin, A. S. Sachrajda, and P. Hawrylak, Phys. Rev. B **72**, 125307 (2005).
[33] Ramin M. Abolfath and Pawel Hawrylak, J. Chem. Phys. **125**, 034707 (2006).